

# Surface hydrogen-palladium studies using a new photopyroelectric detector

Andreas Mandelis and Constantinos Christofides

*Photoacoustic and Photothermal Sciences Laboratory, Department of Mechanical Engineering, and Center for Hydrogen and Electrochemical Studies (CHES), University of Toronto, Toronto, Ontario M5S 1A4, Canada*

(Received 15 February 1990; accepted 28 July 1990)

A new hydrogen gas trace detection principle based on a photopyroelectric solid-state sensor has been developed. The sensor was made of thin commercially available polyvinylidene fluoride (PVDF) pyroelectric film, sputter coated with palladium (Pd). An infrared laser beam (800 nm) served to produce ac voltages due to the photopyroelectric effect. Exposure to hydrogen gas was shown to produce a differential signal between the Pd and reference electrodes. Accumulated experimental evidence has led us to tentatively attribute the detection principle to the adsorption, dissociation, and absorption of hydrogen molecules on the Pd surface, which caused a shift on the PVDF pyroelectric coefficient, due to electrostatic interactions of  $H^+$  ions with the PVDF polar molecular system at the Pd-PVDF interface. A quantitative interpretation of the hydrogen partial pressure dependence of the differential signal has been achieved using simple gas-solid interaction theory and the combination of the Langmuir isotherm with photopyroelectric theory. The new detector could become an excellent tool for surface science studies under ultrahigh vacuum, especially at low temperatures where other sensors do not exhibit good performance.

## I. INTRODUCTION

In recent years, a considerable research effort has been directed toward the development of hydrogen gas detectors. A pyroelectric gas sensor based on dc surface temperature changes due to heats of adsorption-desorption following thermal ramping of the sensor, has also been reported.<sup>1</sup> This paper describes the development of a novel, fast, reversible, sensitive, durable, and simple thin-film photopyroelectric ( $P^2E$ )<sup>2</sup> solid-state sensor for the detection of minute concentrations of hydrogen gas, with distinct advantages over other sensors under STP conditions.<sup>3</sup>

## II. EXPERIMENT

As is well known, poled polyvinylidene fluoride (PVDF) thin films ( $\beta$  phase) exhibit strong pyroelectricity, i.e., a potential difference is generated in the direction of poling between the two metallized electrode surfaces which sandwich the pyroelectric film when a temperature change is induced within the pyroelectric layer.<sup>4</sup> The design of a hydrogen sensor fabricated from such a pyroelectric thin film has become feasible owing to the possibility of depositing a variety of thin metal electrode coatings on PVDF. In this work, PVDF was sputter coated with Pd metal, which can adsorb and subsequently absorb hydrogen gas molecules<sup>5</sup> preferentially in the presence of other ambient gases. The Pd-PVDF film was placed in a standard Inficon<sup>TM</sup> housing as described elsewhere.<sup>6</sup> Our hypothesis was that, upon establishing an ac steady-state temperature field within the pyroelectric electret by amplitude-modulated laser irradiation followed by absorption and photothermal energy conversion, any changes in the pyroelectric generation mechanism(s) in the PVDF, due to interactions with the Pd-absorbed hydrogen, would be registered as changes in the observed  $P^2E$  signal thus yielding a hydrogen sensor.

The signal generation and analysis set up of the  $P^2E$  sensor

is described in Fig. 1(a). The instrumentation consisted of an RCA GaAlAs laser diode powered by an ac current supply. The output laser beam, 4-mW *p-t-p* multimode at  $\sim 800$  nm, was directed to a three-way fiber-optic coupler where it was split at approximately 16%, 34%, and 50% [see Fig. 1(b)]. Only a small fraction of the electrode areas was illuminated. The spot sizes were approximately 0.8 mm in diameter, and could be controlled by moving the optical fibers close to, or away from, the metallized surface. The 16% intensity fiber-optic channel was directed to a photodiode (PD) whose output was then sent to the "monitor" input of the home-made laser current supply for preamplification and feedback control of the laser current, as well as for synchronous lock-in detection. The feedback control consisted of using this reference signal to correct for temporal intensity variations in the modulated laser beam. Light absorption and optical heating always occurred entirely within the metal (Al-Ni) electrode at the back surfaces of the active and reference PVDF films. These surfaces were isolated from contact with any ambient  $H_2$  gas by sealing the optical fiber entrance holes with vacuum grease. The metallized PVDF film is opaque to the infrared laser wavelength ( $\sim 800$  nm) so that sensor operation was in the photopyroelectric saturation regime, independent of the optical absorption properties of the coated PVDF.<sup>7</sup> In the geometry of Fig. 1(b), the ac  $P^2E$  detector signals from a 28- $\mu$ m-thick PVDF film, on which a thickness of Pd  $\sim 130$  Å had been deposited by sputtering (henceforth designated "unit A"), and from a similar reference PVDF film first covered with the standard Pennwalt 200-Ni 600 Å Al ("unit B"), were bandpass-filtered and preamplified by two low noise voltage preamplifiers. The amplified signals were then connected to a double-input oscilloscope for visual display, and to two lock-in analyzers, designated units 1 and 2 [see Fig. 1(a)]. The lock-in analyzers were referenced by the ac laser current supply. The output of lock-in 2 was connected to lock-in ampli-

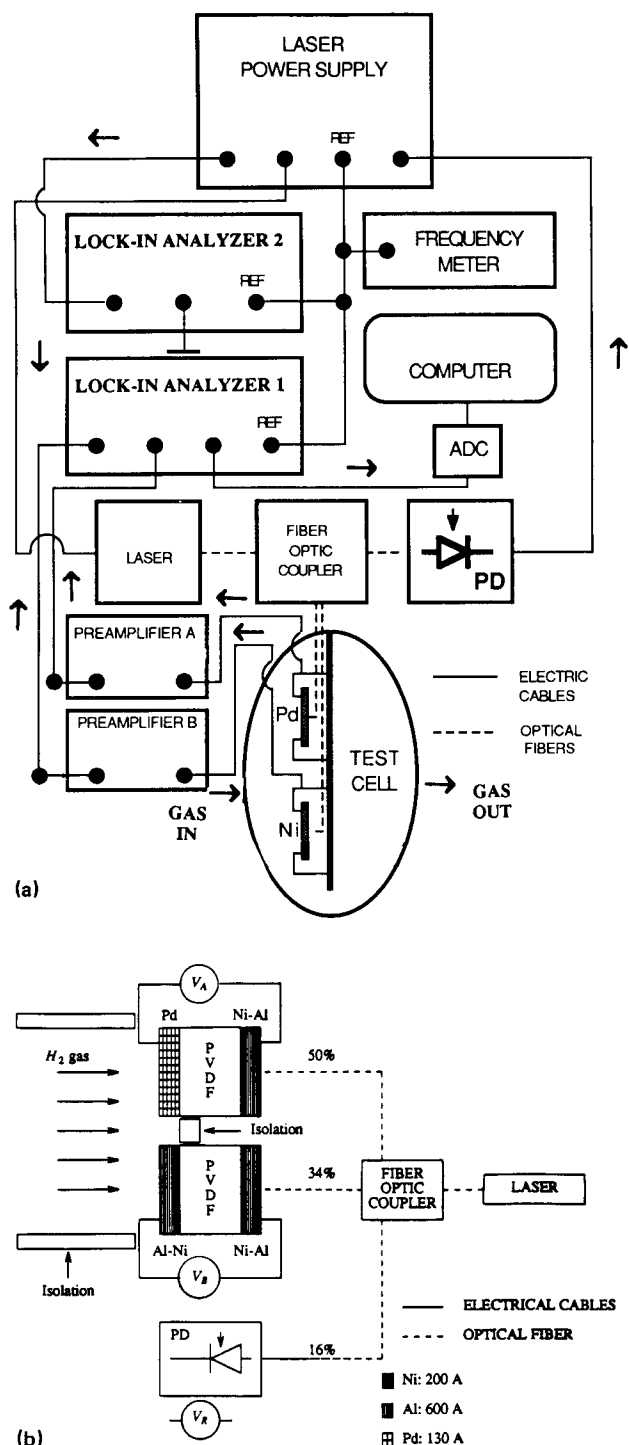


FIG. 1. (a) Schematic diagram of the photopyroelectric detector setup. (b) The Pd-PVDF and Al-Ni-PVDF electrodes of the photopyroelectric detector.

filer 1, which was equipped with a ratio option, allowing a normalized function output:  $|\Delta S| = |V_A - V_B|/|V_R|$ , where  $V_A$  is the voltage output of the Pd-PVDF (active) sensor,  $V_B$  is the voltage generated by the Ni-Al-PVDF (reference) detector, and  $V_R$  is the ac laser power reference output obtained from the photodiode PD. In our case, the modulation of the beam intensity resulted in harmonic

changes in  $\Delta T$ , which subsequently gave rise to the synchronous ac voltages  $V_A$  and  $V_B$ . From the above definition of  $\Delta S$ , the normalized output differential signal between the Pd-PVDF and the Ni-Al-PVDF P<sup>2</sup>E detectors may be written as

$$\Delta S(f) = \frac{1}{V_R} \frac{AR}{z_0 C_v} [\Delta H_{Pd}(f) P_{Pd} - \Delta H_{Ni-Al}(f) P_{Ni-Al}], \quad (1)$$

where  $A$  is the total pyroelectric film area, and  $C_v$  is the PVDF volume heat capacity.  $R$  is given by the relation:  $R = [(1/R_p) + (1/R_A)]^{-1}$ , where  $R_p$  and  $R_A$  are the resistance of the of the pyroelectric capacitor and of the preamplifier input, respectively.  $z_0$  is the thickness of the pyroelectric film.  $\Delta H_{Pd}$  and  $\Delta H_{Ni-Al}$  are the net heat fluxes into the Pd-PVDF and Al-Ni-PVDF P<sup>2</sup>E devices, respectively, and  $P_{Pd}$  and  $P_{Ni-Al}$  are the pyroelectric coefficients of the Pd and Ni-Al coated PVDF films, respectively.  $f$  is the laser diode current modulation frequency ( $\approx 20$  Hz). The lock-in output channels were connected to a computer, through the ports of an A/D converter, for data storage and analysis of the ratioed output signal amplitude,  $\Delta S$ .

Since the heat flows into the P<sup>2</sup>E devices from the laser beams were not very different, the differential voltage was very small under equal preamplifier gains. The magnitude of  $\Delta S$  was further minimized ( $\Delta S \approx 0$ ) at the beginning of each experiment by a judicious choice of gain on the preamplifiers, prior to introduction of the gas into the test cell. In fact, according to Eq. (1) the minimizing of  $\Delta S$  ( $\Delta S \rightarrow 0$ ) led to:  $\Delta H_{Pd} P_{Pd} \approx \Delta H_{Al} P_{Ni-Al}$ . Thus, before the introduction of H<sub>2</sub> into the test cell the differences between the unequal net heat fluxes,  $\Delta H_{Pd}$  and  $\Delta H_{Ni-Al}$ , were eliminated choosing appropriate preamplifier gains. On the other hand, in the absence of H<sub>2</sub> gas ( $[H] = 0$ ), the pyroelectric coefficients of the Pd and Ni-Al coated PVDF films may be assumed identical:  $P_{Pd}[0] = P_{Ni-Al}[0]$ . As a result of the above consideration we can write that  $\Delta H_{Pd} = \Delta H_{Ni-Al} \equiv \Delta H$ . The introduction of hydrogen into the test cell does not change the heat fluxes because  $\Delta T(f)$  is solely determined by the infrared laser beams incident on the PVDF back surfaces unexposed to gas flows. It was further observed that the response of the Al-Ni-PVDF reference detector was insensitive to the presence of the H<sub>2</sub> flow. Therefore, adsorption-absorption of H<sub>2</sub> atoms by the Pd and migration of H<sup>+</sup> ions to the Pd-PVDF interface<sup>8</sup> may be expected to affect the pyroelectric coefficient,  $P_{Pd}$ , through electrostatic interactions of the proton electric field in the Pd with the internal PVDF dipole polarization/charge displacement pyroelectric field<sup>9</sup> across the metal-polymer junction interface. The concentration of the H<sup>+</sup> solid solution is expected to depend on the introduced hydrogen concentrations. Thus, for interaction of H<sub>2</sub> gas with Pd to cause an excess differential voltage  $\delta S$ , according to Eq. (1) we have

$$\delta S = Q \Delta H(f) (P_{Pd}[H] - P_{Ni-Al}[H]), \quad (2)$$

where  $Q \equiv (1/V_R) (AR/z_0 C_v)$  is a system constant. However,  $P_{Ni-Al}[H] = P_{Ni-Al}[0] = P_{Pd}[0]$ , due to the observed insensitivity of the Al-Ni electrode surface to the H<sub>2</sub> gas. Equation (2) shows that in the absence of hydrogen gas  $\delta S = 0$ . With the above considerations and upon writing

$\Delta P_{Pd}[H] \equiv P_{Pd}[H] - P_{Pd}[0]$ , Eq. (2) may be modified as

$$\delta S(f; [H]) = Q \Delta H(f) \Delta P_{Pd}[H]. \quad (3)$$

For small departures from the  $P_{Pd}[0]$  value, the derivative of the pyroelectric coefficient  $P_{Pd}$  with respect to the density of adsorbed molecules (or atoms),  $N_H$ , is the  $\Delta P_{Pd}$  variation:

$$\Delta P_{Pd}[H] = \left( \frac{\partial P_{Pd}}{\partial N_H} \right)_{N_H=0} N_H. \quad (4)$$

Using Eqs. (3) and (4), at the saturation regime (i.e.,  $t \rightarrow \infty: N_H \rightarrow N_{H_s}$  and  $\delta S \rightarrow \delta S_s$ ) we can write

$$\delta S_s = Q \left( \frac{\partial P_{Pd}}{\partial N_H} \right)_{N_H=0} \Delta H(f) N_{H_s}. \quad (5)$$

### III. RESULTS AND DISCUSSION

Figure 2 shows the variation of  $\delta S_s$  as a function of  $H_2$  concentration (and pressure) in the range of 40–2000 ppm (4–200 Pa) of hydrogen in  $N_2$  at 20°C. The solid curve shows a Langmuirian behavior given by<sup>2,8</sup>

$$\delta S_s = \delta S_{\max} \left[ \frac{K(T) \sqrt{P_{H_2}}}{1 + K(T) \sqrt{P_{H_2}}} \right], \quad (6)$$

where  $\delta S_{\max}$  is the maximum signal response of the P<sup>2</sup>E detector corresponding to complete surface coverage of hydrogen.  $K(T)$  is a temperature constant equal to  $5 \times 10^{-3} \text{ Pa}^{-1/2}$ , obtained from a best fit of the data in Fig. 2 to Eq. (6). For each experimental point the response time of the P<sup>2</sup>E sensor (defined as the time interval between signal onset and saturation at a given hydrogen pressure) has also been indicated in parentheses.

The good agreement of the data with the Langmuir model is a strong indicator of the sensitivity of the Pd–PVDF P<sup>2</sup>E sensor response to the dissociation of  $H_2$  on the Pd catalyst,

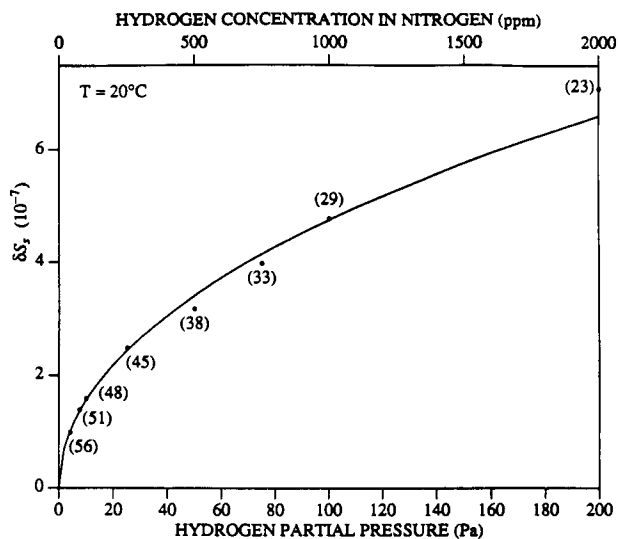


FIG. 2. Variation of output differential signal  $\delta S_s$  as a function of partial pressure (or concentration) of hydrogen. Solid curve: Langmuirian behavior of the photopyroelectric response. Parentheses: Response time at shown hydrogen partial pressure (min).

followed by attainment of equilibrium between adsorbed atomic hydrogen in the Pd bulk and gaseous ambient molecular  $H_2$ . It is therefore concluded that the P<sup>2</sup>E signal is proportional to the density of adsorbed-absorbed hydrogen atoms, as indicated by Eq. (5). Now supportive evidence will be introduced pertinent to the validity of the model of Eqs. (2)–(5) advocating an effect of absorbed hydrogen on  $P_{Pd}$ .

In general, there are four possible sources of the P<sup>2</sup>E signal change in the Pd–PVDF sensor geometry of Fig. 1(b) upon the adsorption of ambient  $H_2$  by the Pd coating and the subsequent appearance of finite bulk density of adsorbed hydrogen atoms:<sup>8</sup> (i) Hydrogen permeation of the Pd–PVDF interface, followed by diffusion in the PVDF bulk affecting the volume heat capacity,  $C_v$ ; (ii) alteration of the Pd–PVDF interfacial stress-strain relationship due to the incorporation of hydrogen atoms/ions in the Pd lattice;<sup>10</sup> (iii) change in the Pd electrode resistivity in the presence of the hydrogen impurities; and (iv) a shift in the value of the pyroelectric coefficient, as per Eqs. (2)–(5). To test some of these possibilities a PVDF film was sputter coated with 285-Å Pd on both sides and pure hydrogen gas was introduced in the cell. The gas was allowed access to the back (illuminated) surface of the sensor via the fiber-optic through-hole. An initial differential signal  $\delta S$  appeared, which returned to the baseline after reaching a maximum, while hydrogen was still flowing. This observation, contrasted with the attainment of time-independent nonzero signal saturation levels in the configuration of the Fig. 1(b), is suggestive (a) of the impermeability of PVDF bulk by hydrogen; and (b) of the invariance of the photothermal pyroelectric signal with the incorporation of hydrogen in the Pd matrix of the illuminated surface (signal return to the same baseline). Next, two PVDF films were coated with 285-Å Pd on oppositely polarized surfaces, in the configuration of Fig. 1(b). They were subsequently exposed to pure hydrogen flow and it was observed that the normalized signal from the positively polarized electrode increased as a function of time, whereas the normalized signal from the negatively polarized electrode decreased in a manner essentially symmetric with respect to baseline (pre-exposure) level. This experiment shows that the P<sup>2</sup>E response is sensitive to the sign of the changes at the PVDF surface next to the Pd layer. This observation suggests that any hydrogen-induced changes in the interfacial stress-strain relation may not be important, as such a variation would result in a mechanical surface area, and thus surface charge density, change, insensitive to the sign of near-the-interface charges. The results are, however, consistent with the presence of charged  $H^+$  ions at the Pd–PVDF interface.<sup>8</sup> In the case of the positively polarized electrode, the additional positive charges (protons) will raise the electrostatic potential of the front surface with respect to the unexposed back surface. This would result in an increased P<sup>2</sup>E voltage, as observed. On the contrary, absorbed protons are expected to neutralize (cancel) the field due to some negative charges at the surface of the negatively polarized electrode, thus lowering the electrostatic potential of the front surface. This would result in the observed decreased P<sup>2</sup>E voltage. A picture involving electrostatic charge com-

penetration by  $H^+$  ions on both metal-polymer interfaces of the symmetric Pd-PVDF-Pd geometry, thus forcing a return of the pyroelectric potential to the baseline as described in the previous experiment, is also consistent with this interpretation.

A change in the Pd resistivity following hydrogen absorption has been known to occur.<sup>5</sup> Fortunato *et al.*<sup>11</sup> have reported a 45% change in the resistance of the Pd-MOSFET (metal-oxide semiconductor field effect transistor) on approaching the  $\alpha \rightarrow \beta$  transition. In the  $H_2$  partial pressure range of our experiments (4–200 Pa), however, a change  $\leq 0.3\%$  is expected.<sup>5</sup> This would result in signal changes much lower than those shown in Fig. 2. A test cell was further prepared in the configuration of Fig. 1(b), with a 45-Å-thick Cu layer between a PVDF film and 285-Å Pd layer of the active detector. Upon repetition of the experiments of Fig. 2 no P<sup>2</sup>E signals could be observed for any hydrogen concentration. This result eliminates electrical resistance change as the signal generation mechanism and corroborates the role of the Pd-PVDF interface as responsible for sensor operation.

At this time it appears that the most likely operating mechanism involves an electrostatic interaction of the absorbed proton field on the metallic side of the interface with the molecular dipole field in the electret, thus affecting the average dipole moment<sup>12</sup> and the total polarization,  $p$ . This model leads to the prediction of a shift of the pyroelectric coefficient,  $P_{Pd}$ , with the Pd absorbed proton density,  $N_H$ :

$$\frac{\partial P_{Pd}}{\partial N_H} = \frac{\partial}{\partial T} \left( \frac{\partial p}{\partial N_H} \right). \quad (7)$$

#### IV. CONCLUSIONS

The main results of our study can be summarized as follows:

(1) Our experimental results suggest that the investigated P<sup>2</sup>E sensor structure can be implemented as a trace hydrogen detector, under ambient conditions or in remote locations without the shortcomings of conventional dc pyroelectric sensors. The room temperature operation capability of the new P<sup>2</sup>E sensor may also be indicative of superior durability over Pd gate MOSFETs, the sensitivity and the response time of which at room temperature are inadequate.

(2) A quantitative interpretation of the hydrogen partial pressure dependence of the differential signal has been

achieved using simple gas-solid interaction theory and the combination of the Langmuir isotherm with photopyroelectric theory.

(3) From the point of view of the basic physics of the photopyroelectric detector operation, a semi quantitative phenomenological understanding has been achieved by showing that the detector response is consistent with elementary adsorption mechanisms in the Pd- $H_2$  system in the low  $H_2$  partial pressure range ( $< 200$  Pa).

(4) the interpretation of our results will be more complete when the physical mechanisms generating the observed response are better understood. The sensor may further help the understanding of the Pd- $H_2$  interaction, as well as the dynamics of the Pd-PVDF and, more generally, the metal-polymer junction electronic behavior.

The hydrogen photopyroelectric detector could also become an excellent tool for surface science studies under UHV, especially at low temperatures where other sensors do not exhibit good performance. In fact UHV studies will also help toward a better understanding of the operating mechanism, because of the highly controlled conditions of the ultrahigh vacuum system. The sensor may further help the understanding of the Pd- $H_2$  interaction, as well as the dynamics of the Pd-PVDF junction electronic behavior. The new photopyroelectric device could also be used in the field of the study of interfacial phenomena such as in the case of polymer/metal interfaces.

<sup>1</sup>J. N. Zemel, B. Kerami, and C. W. Spivak, *Sens. Actuators* **1**, 427 (1981).

<sup>2</sup>A. Mandelis and C. Christofides, *Sens. Actuators* **2**, 79 (1990).

<sup>3</sup>C. Christofides and A. Mandelis, *Appl. Phys. Rev.* **68**, R1 (1990).

<sup>4</sup>KYNAR Piezo Film Technical Manual, Pennwalt Corp., King of Prussia, PA (1983).

<sup>5</sup>F. A. Lewis, *The Palladium/Hydrogen System* (Academic, New York, 1967).

<sup>6</sup>H. J. Coufal, R. K. Grygier, D. E. Horne, and J. E. Fromm, *J. Vac. Sci. Technol. A* **5**, 2875 (1987).

<sup>7</sup>A. Mandelis and M. M. Zver, *J. Appl. Phys.* **57**, 4421 (1985).

<sup>8</sup>I. Lundström, M. Armgarth, and L.-G. Petersson, *CRC Crit. Rev. Solid State Mater. Sci.* **15**, 201 (1989).

<sup>9</sup>G. M. Sessler, in *Electrets*, 2nd ed. *Topics in Applied Physics*, (Springer, Heidelberg, 1987), Vol. 33, Chap. 2.

<sup>10</sup>M. Armgarth and C. Nylander, *IEEE Electron Device Lett.* **EDL-3**, 384 (1982).

<sup>11</sup>G. Fortunato, A. Bearzotti, and C. Caliendo, *Sens. Actuators* **16**, 43 (1989).

<sup>12</sup>F. I. Mopsik and M. G. Broadhurst, *J. Appl. Phys.* **46**, 4204 (1975).